IGSHPA Research Track
Las Vegas, December 6-8, 2022

Accuracy of analytical approaches to thermal response test interpretation

Hae-Rim Oh   Seong-Kyun Kim   Byeong-Hak Park   Ji-Young Baek   Kang-Kun Lee

ABSTRACT

Thermal conductivity obtained via thermal response test (TRT) is one of the essential parameters for the design of shallow geothermal systems, especially a borehole heat exchanger (BHE). During TRT analysis, several factors (e.g., start time of analysis and test duration) could influence the estimated thermal conductivity. In addition, the influence of the factors may be different depending on the characteristics of the borehole and ground. This study investigated the effects of the start time and test duration through numerically generated TRT data under a diversity of environment and BHE information such as the thermal conductivity of grouting and ground. The generated numerical data were analyzed with three analytical approaches having different assumptions about the heat source to interpret the sensitivity of factors in the TRT analysis. By conducting the analytical sensitivity analysis, the importance of determining the appropriate start time and test duration could be emphasized when designing the test.

INTRODUCTION

Thermal conductivity is one of the essential parameters when designing the shallow geothermal system (Marcotte and Pasquier, 2008). A thermal response test (TRT), first presented by Mogensen (1989), has been used to determine the in-situ thermal conductivity, called an effective thermal conductivity. When estimating the effective thermal conductivity using analytical models, it is important to consider a start time and a test duration. Since the response signal is initially influenced by the BHE properties, the start time is intended to ignore the data at the beginning of the test (Stauffer et al., 2013). Gehlin (2002) suggested that the dimensionless time related to the borehole radius, thermal diffusivity, and start time should be greater than 5 for the maximum error to be within 10%. On the other hand, the test duration could affect the cost and accuracy of the test (Raymond et al., 2011). To suggest the appropriate test duration, Beier and Smith (2003) developed a quick method to determine the minimum testing time, and Signorelli et al. (2007) used a numerical simulation to see the effect of test duration according to the ground thermal conductivity. There have been many studies to investigate the influence of the start time and test duration on the effective thermal conductivity. However, although their influences may be different depending on the properties of BHE and ground, few studies have investigated the relationship between the two factors and the experimental environment.

The purpose of this study is to investigate the effect of the start time and the test duration on effective thermal conductivity under various BHE and ground characteristics. First, numerical simulations were performed and the numerically generated data were analyzed using two analytical models having different boundary conditions. Then, the effective thermal conductivity was estimated with varying the start time and test duration. Through the comparison with the thermal conductivity used for the numerical simulation, we investigated how the effective thermal conductivity changed depending on the start time and test duration.

Hae-Rim Oh (ohr0721@snu.ac.kr) is a PhD student at Seoul National University, Seong-Kyun Kim (kskinc@kigam.re.kr) is a researcher at Korea Institute of Geoscience and Mineral Resources, Byeong-Hak Park (bh-park@kaeri.re.kr) is a researcher at Korea Atomic Energy Research Institute, Ji-Young Baek (bjy14114@snu.ac.kr) is a PhD student at Seoul National University, and Kang-Kun Lee (kklee@snu.ac.kr, corresponding author) is a professor of school of earth and environmental sciences at Seoul National University.

DOI: https://doi.org/10.22488/okstate.22.000020

METHODOLOGY

Numerical simulation

Numerical simulations were performed using TOUGH3 (Lawrence Berkeley National Laboratory, Berkeley, CA, USA), which was developed for multi-dimensional fluid and heat flows of multiphase, multicomponent fluid mixtures in porous and fractured media (Jung et al., 2018). The general form of the basic energy balance equations in a porous medium used in TOUGH3 is expressed as follows (Pruess et al., 1999):

$$\frac{d}{dt}\int_{V_n} M dV_n = \int_{\Gamma_n} F \cdot n d\Gamma_n + \int_{V_n} q dV_n \qquad (1)$$

The heat accumulation term *M*, defined as the energy per unit volume, can be rewritten as follows:

$$M = \rho_R c_R T \qquad (2)$$

The conductive heat flux (*F*) is estimated as follows:

$$F = -\lambda \nabla T \qquad (3)$$

Figure 1 shows 2D top view of the model domain. The entire 3D model had a size of 20 m × 20 m × 80 m (length × width × depth) in consideration of the BHE length. The mesh to discretize the model domain was generated using an adaptive gridding technique called a centroidal Voronoi tessellation (CVT) developed by Kim et al. (2015). The mesh generated by the CVT always satisfies the orthogonal shape grid of TOUGH3. The fluid flow was not considered in the simulations. An annual average groundwater temperature of the study site corresponding to 13.0 °C was set as the boundary condition for the entire domain. The basal heat flow of 59.62 mW/m^2 was estimated from the ground thermal conductivity of 2.00 W/m/K and the thermal gradient. Table 1 shows the parameters for the numerical simulation such as the physical properties of BHE and the ground and the experimental conditions. The parameters in Table 1, except for water using the reference value, were derived from actual experimental information. This experiment was conducted according to the guideline (MOTIE, 2019), and the simulation was performed based on this experimental data. We conducted numerical simulations with a time step of 5 minutes.

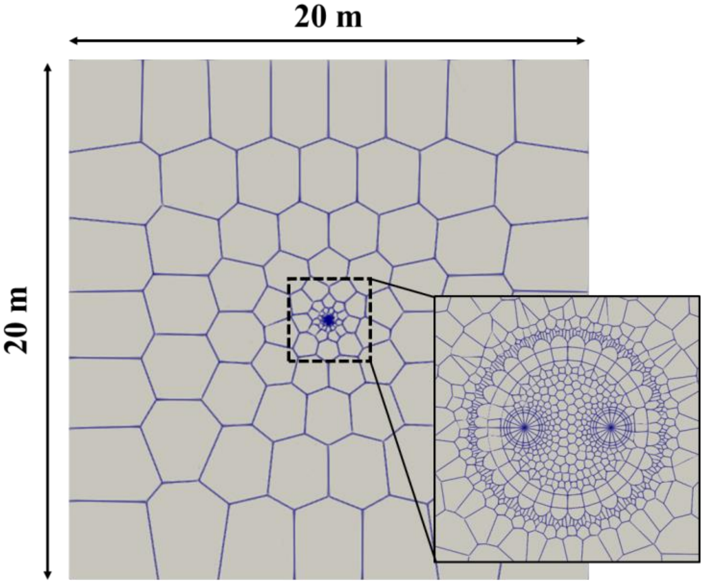

Figure 1 2D top view of the model domain. The domain size is 20 m × 20 m × 80 m (length × width × depth). There are 8,755 elements and 32,814 connections.

Table 1. Model input parameters

Parameters (unit)	Value
Borehole heat exchanger	
Borehole depth (m)	76
Borehole diameter (m)	0.152
U-tube: Polyethylene	
Outer diameter (m)	0.040
Inner diameter (m)	0.036
Grout	
Thermal conductivity (W/m/K)	0.79
Specific heat (kJ/kg/K)	2.00
Heat carrier fluid: Water	
Thermal conductivity (W/m/K)	0.58
Specific heat (kJ/kg/K)	4.20
Ground	
Thermal conductivity (W/m/K)	2.00
Volumetric heat capacity (MJ/m^3/K)	3.55
Experimental conditions	
Heat flow rate per unit length of borehole (W/m)	62.66
Average flow rate of the fluid (L/min)	17.05
Initial temperature (℃)	13.45
Average temperature difference (℃)	4.01

In order to consider the influence of λ_{ground} and λ_{grout}, we generated several numerical data under various conditions (Table 2). λ_{grout} values were additionally assigned as 1.35 (used in Brettmann et al. (2011)), 1.73, and 2.10 W/m/K (used in Choi et al. (2011)), respectively. Considering that the thermal conductivity may vary depending on the ground, λ_{ground} values were set to 1, 2, 3, and 4 W/m/K. Figure 2 shows the mean fluid temperature between the inlet and outlet of BHE in the simulation results.

Table 2. Conditions for data generation under various thermal conductivity of ground and grouting material

Factor	Thermal conductivity of ground (W/m/K)	Thermal conductivity of grouting material (W/m/K)
Ground thermal conductivity	1.00	0.79
	2.00	
	3.00	
	4.00	
Grout thermal conductivity	2.00	0.79
		1.35 (used in Brettmann et al. (2011))
		1.73
		2.10 (used in Choi et al. (2011))

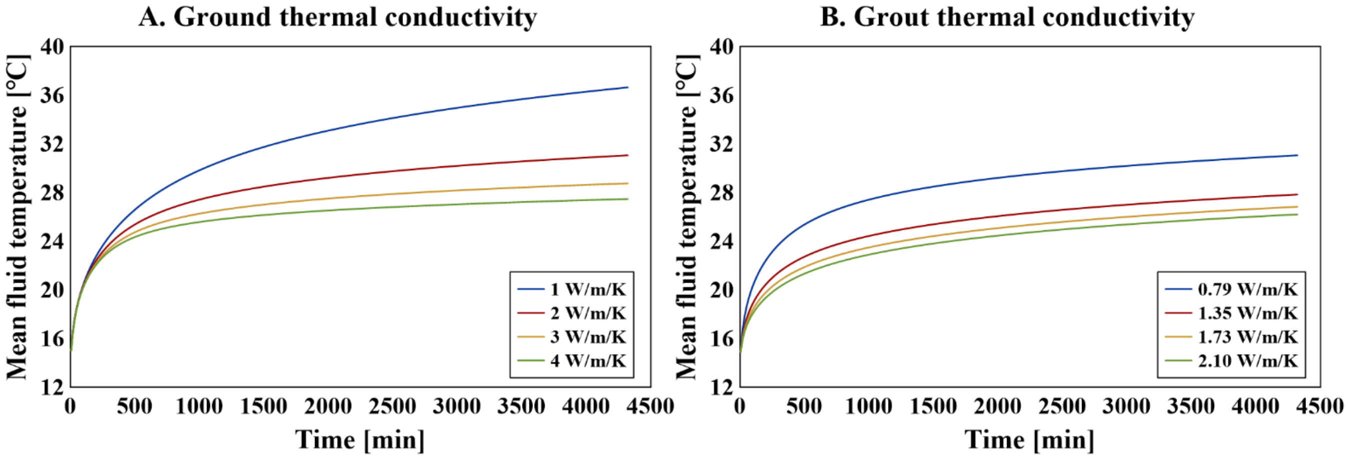

Figure 2 Simulated mean fluid temperature for (a) Ground thermal conductivity and (b) Grout thermal conductivity.

Analytical models

In this study, two analytical models with different assumptions of the heat source were used to estimate the thermal conductivity. Numerically generated data were analyzed by an infinite line source (ILS) model expressed in Equation 4 (Carslaw and Jaeger, 1959).

$$T_f(t) = \frac{q_{tb}}{4\pi\lambda_{eff}}\ln(t) + q_{tb}\left[R_b + \frac{1}{4\pi\lambda_{eff}}\left(\ln\left(\frac{4\alpha t}{{r_b}^2}\right) - \gamma\right)\right] + T_0 \tag{4}$$

The logarithmic approximation of the ILS model can be expressed as a linear regression function as follows (Eklöf and Gehlin, 1996):

$$\frac{dT_f}{d(\ln(t))} = \frac{q_{tb}}{4\pi\lambda_{eff}} \tag{5}$$

λ_{eff} can be determined using Equation 5, and the obtained λ_{eff} is referred to as $\lambda_{\mathrm{ILS\text{-}lin}}$ in this study.

$$\lambda_{ILS-lin} = \frac{q_{tb}}{4\pi}\left(\frac{dT_f}{d(\ln(t))}\right)^{-1} \tag{6}$$

An infinite cylindrical source (ICS) model that extends a line source to a cylindrical source with radius *r* was also used to analyze the numerically generated data. The ICS model can be expressed in Equation 7 (Ingersoll et al., 1954).

$$T_f(t) = T_0 + \frac{q_{tb}}{\pi^2\lambda_{eff}}\int_0^\infty \frac{e^{-\beta^2 \mathrm{Fo}}-1}{J_1^2(\beta)+Y_1^2(\beta)} \times [J_0(R\beta)Y_1(\beta) - J_1(\beta)Y_0(R\beta)]\frac{d\beta}{\beta^2} + q_{tb}R_b \tag{7}$$

Parameter estimation approach. When using the ILS model, the measured temperature data can be fitted by a linear regression method in Equations 5 and 6 or a parameter estimation method (Stauffer et al., 2013). The parameter estimation method was used not only in ILS but also in ICS, which cannot be represented by the linear regression. To estimate thermal parameters, two variables (thermal conductivity and borehole thermal resistance) were obtained when the root mean squared error (*RMSE*) was the minimum. *RMSE* was calculated by changing the variables within the established reference range. Thermal parameters having the minimum *RMSE* were determined at each step. The *RMSE* between the observed and modeled values was given by the following formula:

$$RMSE = \sqrt{\frac{\Sigma_{i=1}^{N}\left(T_{f,model}(t_i) - T_{f,meas}(t_i)\right)^2}{N}} \tag{8}$$

$T_{f,model}$ can be obtained by using ILS and ICS (Equations 4 and 7). $\lambda_{ILS\text{-}par}$ and λ_{ICS} were used as λ_{eff} estimated by each model.

RESULTS

Analytical sensitivity analysis

We set a comparison criterion to quantitatively compare the effect of factors. Kavanaugh (2000) stated that 10% change in thermal conductivity could lead to 4.5–5.8% error of the borehole length, which could lead to a 1% change in cooling capacity and 0.7% change in heating capacity. Based on the results in Kavanaugh (2000), an acceptable change was defined as within 10% in this study.

Effect of start time. To conduct the analytical sensitivity analysis of the start time for the thermal conductivity estimation, the start time was ranged from 0 to 1,000 minutes in 100 minutes' increments. The test duration was fixed at 4,320 minutes. Figure 3 shows the change of the estimated thermal conductivity with the start time. Figure 3a shows the change in λ_{eff} with the start time in the case of λ_{ground}. When comparing λ_{eff} with λ_{num}, the largest differences were shown in the order of λ_{ICS} (-37.50%), $\lambda_{ILS\text{-}par}$ (-34.50%), and $\lambda_{ILS\text{-}lin}$ (-30.49%). These results were obtained when λ_{ground} was the highest at the minimum start time within the analysis range. As the start time increased, the difference between λ_{eff} and λ_{num} decreased. The start time for the difference to reach within 10% increased with increasing λ_{ground}. In these results, the start time had to be at least 600 minutes to have an acceptable difference within 10%.

In the case of λ_{grout} (Figure 3b), the largest differences were also shown in the order of λ_{ICS} (-24.00%), $\lambda_{ILS\text{-}par}$ (-19.00%), and $\lambda_{ILS\text{-}lin}$ (-17.48%). As with the results of λ_{ground}, the difference between λ_{eff} and λ_{num} decreased with increasing the start time. The difference between $\lambda_{ILS\text{-}lin}$ and λ_{num} was the largest when λ_{grout} was 2.10 W/m/K. On the other hand, the differences of $\lambda_{ILS\text{-}par}$ and λ_{ICS} were more than 10% as the maximum when λ_{grout} was 0.79 W/m/K. Considering λ_{grout} of 0.79 W/m/K with the largest change according to the start time, the start time showed a difference within 10% after 300 minutes.

Comparing the results of λ_{ground} (Figure 3a) and λ_{grout} (Figure 3b), λ_{eff} was estimated significantly different from λ_{num} in the early part of the two analysis results. λ_{ground} had a greater effect on the results of start time than λ_{grout}. In our results, the change of λ_{eff} within the analysis range was the greatest having the highest λ_{ground} and the lowest λ_{grout}.

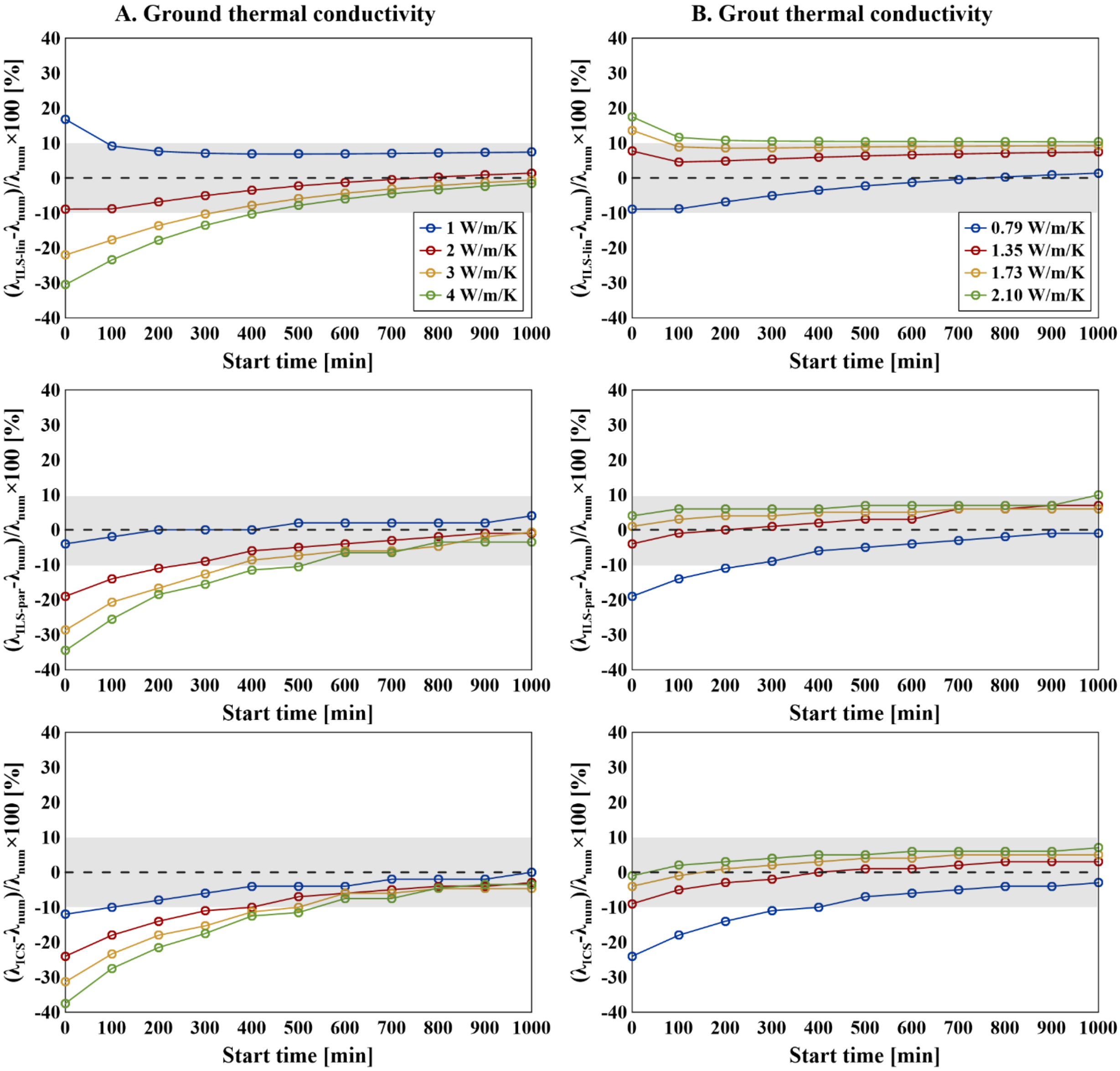

Figure 3 The change in estimated thermal conductivity when the start time is changed from 0 to 1,000 minutes in cases of (a) Ground thermal conductivity and (b) Grout thermal conductivity. The gray area means the section within the acceptable difference of 10%.

Effect of test duration. In the process of the sensitivity analysis, the test duration was changed from 2,880 to 4,320 minutes in 60 minutes' increments. During this analysis, the start time was set at 720 minutes according to MOTIE (2019), and other factors were not changed. Figure 4 shows the change in estimated thermal conductivities according to the test duration.

In case of λ_{ground} (Figure 4a), the maximum difference between $\lambda_{ILS\text{-}lin}$ and λ_{num} was shown in the order of λ_{ICS} (-10.50%), $\lambda_{ILS\text{-}par}$ (-10.00%), and $\lambda_{ILS\text{-}lin}$ (8.13%). The largest differences of λ_{ICS} and $\lambda_{ILS\text{-}par}$ were greater than 10% when λ_{ground} was 3 or 4 W/m/K. At the case of λ_{ground} of 3 W/m/K, the largest difference was calculated in the initial part of the analysis range, and it was determined in the middle part when λ_{ground} was 4 W/m/K. With a few exceptions, the estimates were generally within the acceptable range. Figure 4b shows the change of λ_{eff} according to the test duration in the case of λ_{ground}. Except for $\lambda_{ILS\text{-}lin}$ (10.55%), the largest differences of $\lambda_{ILS\text{-}par}$ and λ_{ICS} were smaller than the comparison criterion of 10%. Considering the specific test duration that exceeded 10%, it was confirmed that the longer the test duration, the better.

As shown in Figure 4, the estimated thermal conductivities are relatively constant compared to the results of start time (Figure 3). That is, even if the test duration was increased, the difference from λ_{num} did not change significantly. Therefore, it seems difficult to mention that there was a noticeable change in the estimated thermal conductivity according to the test duration within the analysis range in this study.

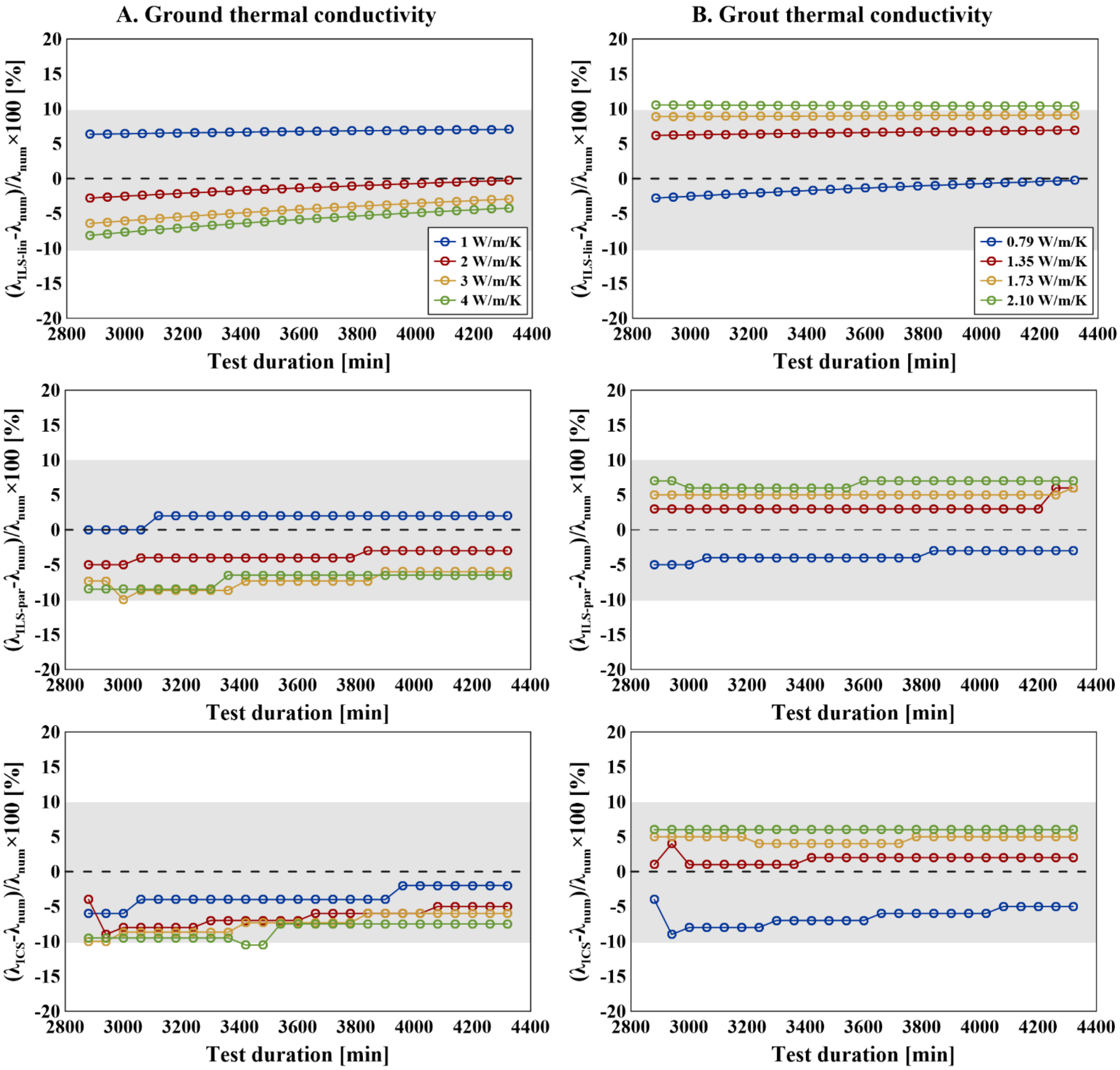

Figure 4 The change in estimated thermal conductivity when the test duration is ranged from 2,880 to 4,320 minutes in cases of (a) Ground thermal conductivity and (b) Grout thermal conductivity. The gray area means the section within the acceptable difference of 10%.

CONCLUSION

This study conducted the analytical analysis to investigate the effect of start time and test duration on TRT interpretation when the thermal properties of BHE and ground were different. First, several numerical simulations were conducted to generate experimental data with different thermal conductivity of the grouting material and ground. Then, three commonly used analytical methods were used to estimate the thermal conductivity, and the influence of start time and test duration on the methods used was compared. The results showed that the start time could have more influence on the effective thermal conductivity more than the test duration. In particular, the ground thermal conductivity had a greater impact on the start time. In these results, the effective thermal conductivity could be appropriately estimated when the start time was greater than 600 minutes and the test duration was greater than 3,540 minutes (with the start time of 720 minutes). However, it is difficult to generalize these results because there are a lot of factors related to the characteristics of the ground and BHE. Other factors should be considered to suggest the appropriate start time and test duration. These results suggest that it is important to consider BHE and ground characteristics for accurate TRT analysis. This analysis is expected to help design the BHE more efficiently.

ACKNOWLEDGMENTS

This work was supported by the National Research Foundation of Korea (NRF) grant funded by the Korea government (MSIP) (No. 2022R1A2C1006696). This work was also supported by the Institute for Korea Spent Nuclear Fuel (iKSNF) and National Research Foundation of Korea (NRF) grant funded by the Korean government (Ministry of Science and ICT, MSIT) (Grant number: 2021M2E1A1085200).

NOMENCLATURE

V_n = Arbitrary subdomain bounded by the closed surface Γ_n (m^3)
n = Normal vector on the surface element $d\Gamma_n$ pointing inward into V_n (-)
F = Heat flux (mW/m^2)
q = Heat sources or sinks (J/s)
M = Heat accumulation term (J/m^3)
ρ = Density (kg/m^3)
c = Specific heat (J/kg/K)
λ = Thermal conductivity (W/m/K)
T = Temperature (°C)
q_{tb} = Heat flow rate per unit length of the borehole (W/m)
r = Radial distance (m)
α = Thermal diffusivity (m^2/s)
T_o = Undisturbed ground temperature (°C)
t = Time (s)
γ = Euler's constant (=0.5722) (-)
R_b = Effective borehole resistance (mK/W)
R = Dimensional cylindrical radius ($=r/r_0$) (-)

J_n = Bessel function of the first kind of order *n*
Y_n = Bessel function of the second kind of order *n*

Subscripts

eff = Effective
f = Fluid
b = Borehole wall
model = Modeled
meas = Measured
ILS = Infinite line source (ILS) model
ICS = Infinite cylindrical source (ICS) model
lin = Linear regression method
par = Parameter estimation method
grout = Grouting material
ground = Ground
num = Numerical model

REFERENCES

Beier, R.A. and Smith, M.D. 2003. *Minimum duration of in-situ tests on vertical boreholes*. ASHRAE Transactions, 109, 475.

Brettmann, T. and Amis, T. 2011. *Thermal conductivity evaluation of a pile group using geothermal energy piles*. In Geo-Frontiers 2011: Advances in Geotechnical Engineering (pp. 499-508).

Carslaw, H. S. and Jaeger, J. C. 1959. Conduction of heat in solids. Oxford, UK: Oxford University Press.

Choi, J. M., Lee, C., Park, M., Kang, S. H. and Choi, H. 2011. *Numerical simulation for thermal response test performance in closed-loop vertical ground heat exchanger*. Science China Technological Sciences, 54(7), 1668-1673.

Eklöf, C. and Gehlin, S. 1996. *TED: a mobile equipment for thermal response test*. Master's Thesis, 1996: 198E, Luleå University of Technology, Sweden.

Gehlin, S. 2002. *Thermal response test: method development and evaluation*. PhD Thesis, Luleå University of Technology, Sweden.

Ingersoll, L. R., Zabel, O. J. and Ingersoll, A. C. 1954. Heat conduction with engineering, geological, and other applications. New York, USA: McGraw-Hil.

Jung, Y., Pau, G. S. H., Finsterle, S. and Doughty, C. 2018. *TOUGH3 user's guide*. University of California, Berkeley.

Kavanaugh, S. P. 2000. *Field tests for ground thermal properties--methods and impact on ground-source heat pump design*. Univ. of Alabama, Tuscaloosa, AL (US).

Kim, S. K., Bae, G. O. and Lee, K. K. 2015. *Improving accuracy and flexibility of numerical simulation of geothermal heat pump systems using Voronoi grid refinement approach*. Geosciences Journal, 19(3), 527-535.

Marcotte, D. and Pasquier, P. 2008. *On the estimation of thermal resistance in borehole thermal conductivity test*. Renewable energy, 33(11), 2407-2415.

Mogensen, P. 1983. *Fluid to duct wall heat transfer in duct system heat storages*. Document-Swedish Council for Building Research, (16), 652-657.

MOTIE. 2019. *Standards of Support, Installation, and Management of New and Renewable Energy system*. South Korea.

Pruess, K., Oldenburg, C. M. and Moridis, G. J. 1999. *TOUGH2 user's guide version 2* (No. LBNL-43134). Lawrence Berkeley National Lab.(LBNL), Berkeley, CA (United States).

Raymond, J., Therrien, R., Gosselin, L. and Lefebvre, R. 2011. *A review of thermal response test analysis using pumping test concepts*. Groundwater, 49(6), 932-945.

Signorelli, S., Bassetti, S., Pahud, D. and Kohl, T. 2007. *Numerical evaluation of thermal response tests*. Geothermics, 36, 141-166.

Stauffer, F., Bayer, P., Blum, P., Giraldo, N. M. and Kinzelbach, W. 2013. Thermal use of shallow groundwater. CRC Press.